ELSEVIER

Polymer 41 (2000) 1175–1182

polymer

NMR investigation of phase transitions in polyethylene in the vicinity of the hexagonal high pressure phase

M. de Langen*, K.O. Prins

Van der Waals-Zeeman Institute, University of Amsterdam, Valckenierstraat 65, 1018 XE Amsterdam, The Netherlands

Received 16 July 1998; received in revised form 25 January 1999; accepted 18 March 1999

Abstract

The location of the hexagonal crystalline phase of polyethylene in a *pT*-diagram, occurring at high pressure and high temperature, was determined from proton-NMR spin–lattice relaxation rates and found to be in good agreement with the results obtained with other techniques. Hexagonal and orthorhombic crystalline components as well as the amorphous part in a sample at high pressure can clearly be distinguished by deuteron NMR spectra. The changes in these components were followed as a function of temperature at various pressure values, showing the coexistence of orthorhombic and hexagonal crystalline materials during crystallization. © 1999 Elsevier Science Ltd. All rights reserved.

Keywords: Polyethylene; Phase transitions; NMR

1. Introduction

Solid polyethylene (PE) is a semi-crystalline material, in which at least some part of the solid is amorphous. Both the crystalline and the amorphous parts are often combined in some form of lamellar structure, of which the exact nature depends on conditions and sample history. The degree of crystallinity, sizes of the amorphous and the crystalline domains and interfacial structures between the two fractions have been subjects of research for many years.

Under normal conditions crystalline PE has an orthorhombic structure. In 1974, using DTA and dilatometry experiments, Bassett and Turner [1,2] discovered that at high pressure (above about 3500 bar), a transition to a phase, unknown until that time, occurs below the melting transition. Later, X-ray experiments [3] have shown that this new phase has a hexagonal crystal structure. An interesting phenomenon involving the hexagonal phase is that the PE that has been crystallized at high pressure via the hexagonal phase attains the extended chain morphology, while the PE normally shows a folded chain morphology after crystallization from the melt at ambient pressure.

The object of the study in this and the two next papers [4,5] is the behaviour of PE in both crystal structures and in the vicinity of phase transitions near the hexagonal phase, with emphasis on the chain dynamics. Especially for this latter aspect, the use of nuclear magnetic resonance (NMR) as an experimental technique is particularly well suited. Motional frequencies that can be observed in PE using an NMR range from about 10^9 Hz (using spin–lattice relaxation times) to about 10^{-3} Hz (using two-dimensional exchange experiments). This information originates from the local interactions of the nuclei. In the present investigation of the properties of solid PE, we make use of the magnetic dipole–dipole coupling between proton spins and of the electric quadrupolar interaction of the deuteron. The first is used with standard UHMWPE samples and the latter with a deuterated PE sample. Since molecular motion changes considerably in the vicinity of phase transitions, NMR is also an excellent tool to study phase transitions. It has been used to study the orthorhombic phase [6–15] and the melting transition [16,17], for the conventionally crystallized material [18–20], high pressure or solution crystallized material [21–23] (extended chain), and oriented material [14,24,25]. Practically all of these studies have been performed at ambient pressure only.

The purpose of this paper is to show how the results of our NMR investigation are used to construct the phase diagram and to determine amorphous, orthorhombic and hexagonal fractions in PE as a function of temperature and pressure. More detailed information on the chain dynamics in each of the phases and full discussions of both the NMR techniques

* Corresponding author. Tel.: +31-205256334; fax: +31-205255788.
E-mail address: langen@phys.uva.nl (M. de Langen)

PII: S0032-3861(99)00248-7

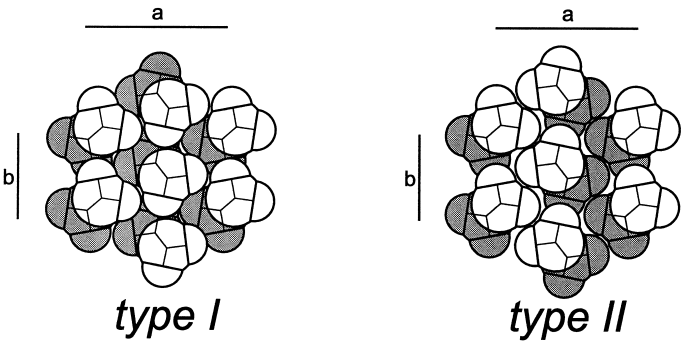

Fig. 1. The orthorhombic unit cell viewed along the *c*-axis ordered correctly (type I) and incorrectly (type II).

and the NMR results will be presented in the next two papers on the orthorhombic and hexagonal phases, respectively.

2. Experimental

2.1. NMR spectrometer and high-pressure probe

The proton-NMR and deuteron-NMR experiments were performed (at 180 and 27.3 MHz, respectively) in a home-built pulse spectrometer using a superconducting magnet ($B = 4.2$ T, bore 13 cm, Oxford Instruments). For the rather extreme conditions of pressure and temperature required in this project, we developed a titanium high-pressure (10 kbar), high-temperature NMR probe, which is described in detail elsewhere [26]. The temperature control allows experiments from room temperature up to 600 K, with an accuracy of 0.1 K.

The PE samples are pressurized using an inert fluid perfluoroether (Hostinert-272, Hoechst AG). The pressure is measured with an accuracy of 5 bar using manganine resistance cells.

2.2. Sample

The material used in the proton-NMR experiments is UHMWPE, Hostalen GUR 403[1], kindly provided by Hoechst AG. The crystallinity of the untreated material is about 80%, as determined at room temperature from proton-NMR echoes. A fully deuterated linear PE sample ($M_w = 100\,000$; $M_w/M_n = 10$; Merck Darmstadt), made available by Prof. H.W. Spiess, was used in the deuteron-NMR experiments.

2.3. NMR methods

The deuteron-NMR spectra was obtained by Fourier transforming the free induction decays following a quadrupole echo pulse sequence, using an inter-pulse spacing of 40 μs. The spin-lattice relaxation times were determined using the saturation recovery method. The spin-locking field used in the $T_{1\rho}^{H}$ experiments is equivalent to a frequency of 100 kHz. A more detailed description of the experimental procedures can be found in the next paper [4].

2.4. Crystal structure

The orthorhombic crystal structure of PE, in which the chains are arranged in their all-*trans* conformations, was first reported by Bunn [27,28]. The unit cell of PE consists of two pairs of CH_2 units with the orientations of the all-*trans* planes almost perpendicular as shown on the left-hand side in Fig. 1. In this figure part of the orthorhombic lattice is shown viewed perpendicular to the *ab*-plane. In the orthorhombic lattice, the two hydrogen atoms belonging to the same CH_2 group have different surroundings, due to the unequal lengths of the *a* and *b* axes. The light-coloured CH_2 groups in Fig. 1 are positioned above the darker groups, showing the corresponding ordering in the *c*-direction. This is the ordering that is also expected from the close packing considerations. We note that, in principle, the ordering of an orthorhombic PE crystal could also be as shown on the right hand side of Fig. 1. In the literature both the ordering of type I [27,29,30] and the ordering type II [28,29,31,32] are used. However, all of these references refer back to the work of Bunn. The confusion in the literature is probably caused by a partly incorrect figure in Ref. [28]. It is obvious from Fig. 1 that the orthorhombic structure does not allow much freedom for the PE chains. Therefore, near room temperature the motion of these chains is almost completely limited to small angle reorientations. However, slow longitudinal chain diffusion has been observed in ^{13}C-NMR, 2D-exchange and spin–lattice relaxation experiments [10,11,33].

The hexagonal nature of the high pressure phase of PE has been found by Bassett et al. [3]. Using X-ray measurements and knowledge of the specific volume, they concluded that the average interval between CH_2 units in the *c*-direction is reduced from 2.53 to 2.45 Å. This means that the PE chains in the hexagonal structure are not in the all-*trans* conformation, but must contain some disorder.

[1] Hoechst AG, Frankfurt am Main, UHMWPE, $M_\eta = 5.6 \times 10^6$ g/mol, no additives.

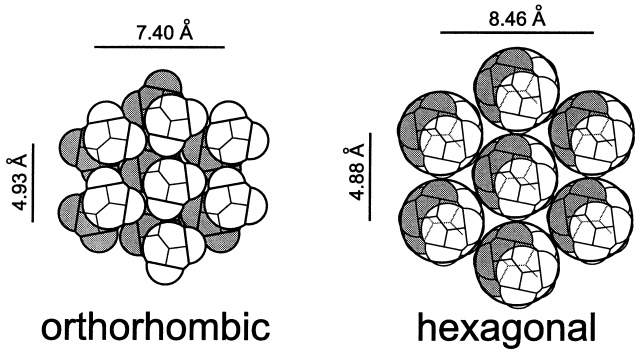

Fig. 2. Schematic drawing of the orthorhombic and hexagonal crystal structures. A slice of the crystal is viewed along the chain direction.

This was confirmed by Yasuniwa et al. [34]. These authors observed no reflections in their X-ray measurements originating from order in the *c*-direction. We have found no reports that give conclusive evidence on the exact nature of the disorder of the chains. It is very likely that a number of gauche defects is involved, but some fraction of the disorder may well originate from the so-called soft twists.

A PE unit cell with the hexagonal structure is shown in Fig. 2. It shows that the hexagonal lattice can be thought to coincide with an orthorhombic point lattice with different lengths of its *a* and *b* axes. Therefore, at the phase transition from orthorhombic PE to hexagonal PE, the crystal lattice can be thought to change its lattice parameters *a* and *b* to the values given in Fig. 2 while at the same time the chain conformation gets disordered. The larger space per chain in the hexagonal phase allows rapid motion about the *c*-axis and rapid diffusion of the chains along the *c*-direction.

3. Results and discussion

As will be shown in the following two papers, we have investigated the orthorhombic and hexagonal phases of PE. The data obtained from various NMR experiments was used to obtain information on the molecular motion in each of these phases. By knowing which motional processes are responsible for the results of the different NMR experiments it is possible to use these NMR methods to perform an exploration of the phase diagram. In this paper the dependences of NMR data on temperature and pressure, and in particular the changes in these properties occurring in the vicinity of the phase transitions will be examined closely. The molecular motions in the PE crystal change their rates discontinuously near phase transitions. In going from one phase to another, new types of motion start to emerge while others become less significant for the observed properties.

3.1. Phase transitions studied using spin–lattice relaxation data

The phase diagram can be established by recording the results from various NMR experiments along isobaric paths through the phase transitions at several pressure values. The experimentally easiest indicators for the positions of the phase transitions are the proton spin–lattice relaxation times T_1^H and $T_{1\rho}^H$ and the deuteron spin–lattice relaxation time T_1^D. Fig. 3 shows the behaviour of T_1^H (at 180 MHz) at a pressure of 1 bar. The most obvious features of the temperature dependence of T_1^H are the minimum at 283 K, the steady increase in a large interval of temperature and the enormous decrease of the relaxation time on approaching the melting transition at 408 K. The point where the steep drop of the T_1^H values stops is the melting point at ambient pressure. As will be discussed in the next paper [4], proton spin–lattice relaxation in the orthorhombic phase is caused by spin diffusion to rapidly relaxing spins in the amorphous and interfacial fractions and at end groups and crystal defects. As this mechanism enters the extreme narrowing regime, T_1^H increases with temperature. Well below the phase transition,

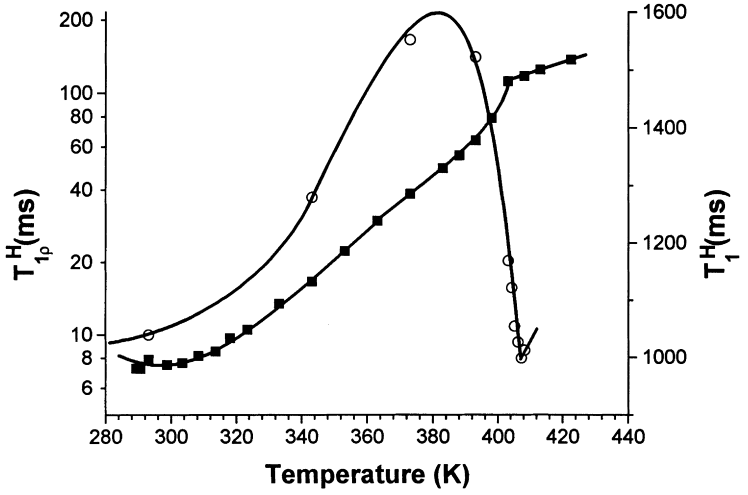

Fig. 3. Temperature dependence of $T_{1\rho}^H$ and $T_{1\rho}^H$ of PE (Hostalen GUR 403) at ambient pressure. The open circles show the behaviour of T_1^H and the filled squares that of $T_{1\rho}^H$.

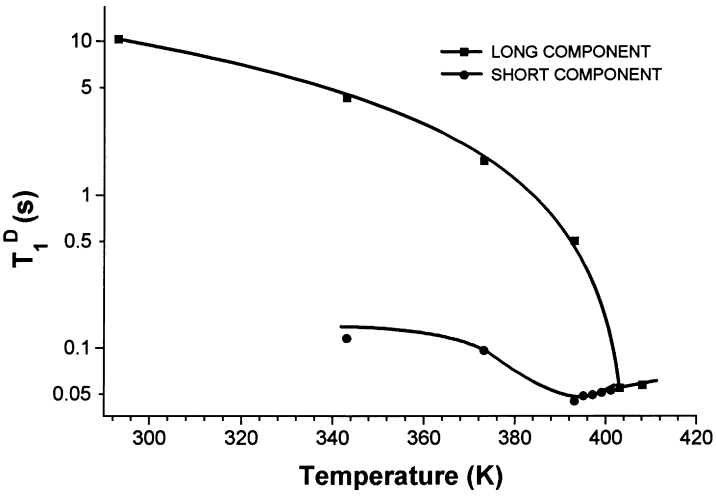

Fig. 4. Temperature dependence of T_1^D of deuterated PE at ambient pressure.

torsional reorientations of the CH_2 groups about the chain axes, which are the mechanism for $T_{1\rho}^H$ and for T_1^D in the crystalline component are neither fast nor large enough to be a T_1^H mechanism.

This situation changes in the temperature region close to the transitions to either the liquid or the hexagonal phase. Apparently, the reorientational motion of the CH_2 groups becomes less restricted. On increasing the temperature, the reorientation angles increase and the motion gradually becomes quasi-isotropic, while the reorientation rate increases rapidly. This can be seen most clearly in Fig. 4, showing the temperature dependence of the deuteron spin–lattice relaxation time T_1^D, also at 1 bar. This relaxation time shows a steep decrease of the relaxation time in the crystalline part (the long relaxation time component [4]), when the melting transition is approached. The quasi-isotropic motion of the CH_2 groups and the speeding up of the reorientation now also have become a mechanism (in its slow-motion regime) for proton spin–lattice relaxation for all CH_2 groups in the chain. This is what causes the rapid decrease of T_1^H near the phase transition.

The behaviour of the rotating-frame relaxation time $T_{1\rho}^H$ at

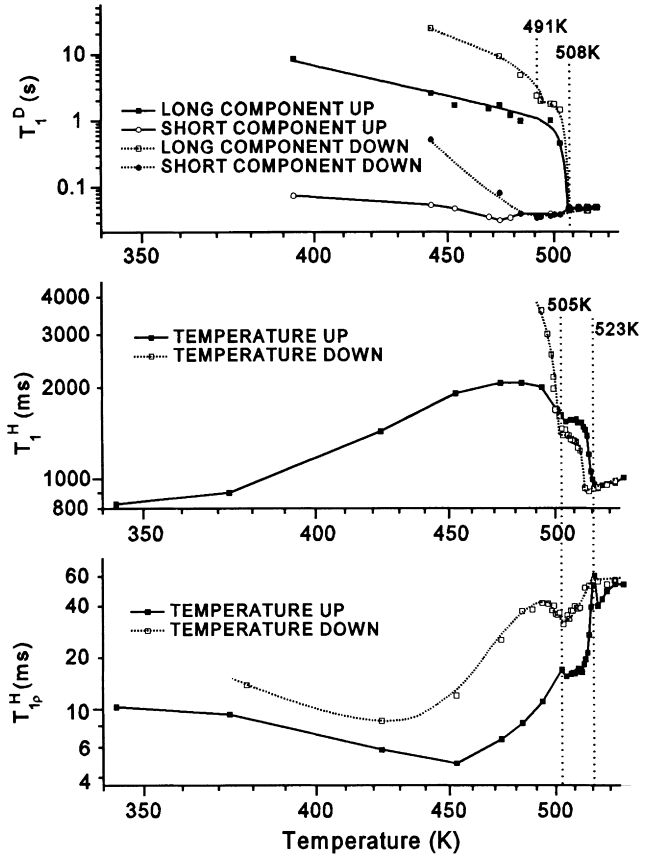

Fig. 5. Temperature dependence of relaxation times at 4900 bar.

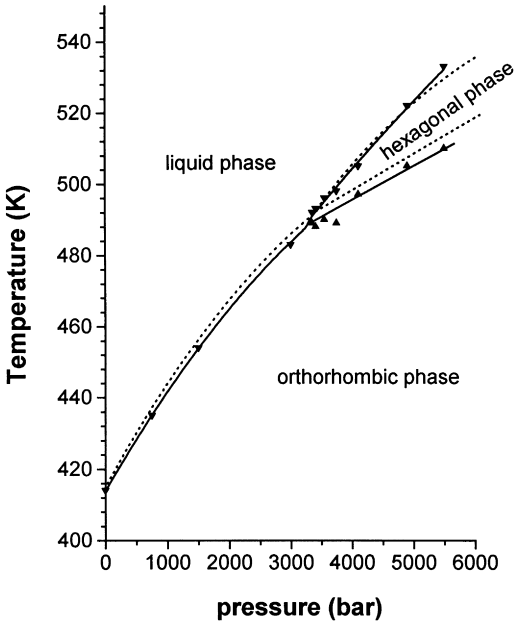

Fig. 6. The phase diagram of PE. Our proton-NMR data (solid lines) on UHMWPE compared to DTA/DSC data (dotted lines) of Hikosaka et al. [32].

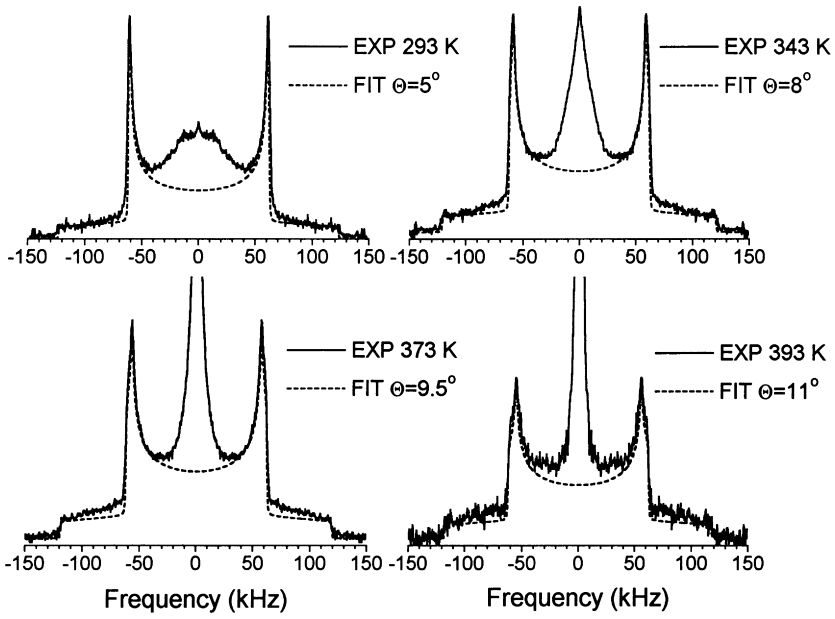

Fig. 7. Temperature dependence of deuteron NMR line shapes at ambient pressure. Angles Θ result from fits using a model of fast reorienting CD_2 groups (see next paper [4]).

1 bar is also shown in Fig. 3. As will be discussed in the next paper [4], the value of $T_{1\rho}^{H}$ increases as a consequence of the increasing reorientation rate of the CH_2 groups, until at the melting transition the slope of its temperature dependence changes discontinuously. The temperature dependences of T_1^H and $T_{1\rho}^H$ shown in Fig. 3 were recorded during different sessions on samples with a different history. As a result, the melting points determined from these experiments occur at slightly different temperature values. In relation to the T_1^D data in Fig. 4 we note that for deuterated PE, the melting point is about 6 K lower than for non-deuterated PE. This effect has been observed previously by Hentschel et al. [19].

At high pressure more discontinuities due to phase transitions are visible because of the presence of the hexagonal phase. The results of T_1^H, $T_{1\rho}^H$ and T_1^D experiments at 4900 bar are collected in Fig. 5. Using these discontinuities, we have determined the positions of the phase transitions at several pressure values. The information from T_1^H and $T_{1\rho}^H$ data was used to construct the pT-phase diagram for PE, which is shown in Fig. 6. In this phase diagram the areas where PE is orthorhombic, hexagonal or liquid are shown, up to a pressure of about 6 kbar. The positions of the phase transition lines are determined by fitting the second-order polynomial curves through the experimentally observed phase transition points. For only this, the points are taken from isobaric paths at increasing temperature. The paths with decreasing temperature have also been recorded but because one would have to wait for infinitely long times in order to obtain the correct equilibrium crystallization temperature, the phase transitions detected in these paths show up at too low values of the temperature. The phase diagram obtained from our NMR experiments is in good

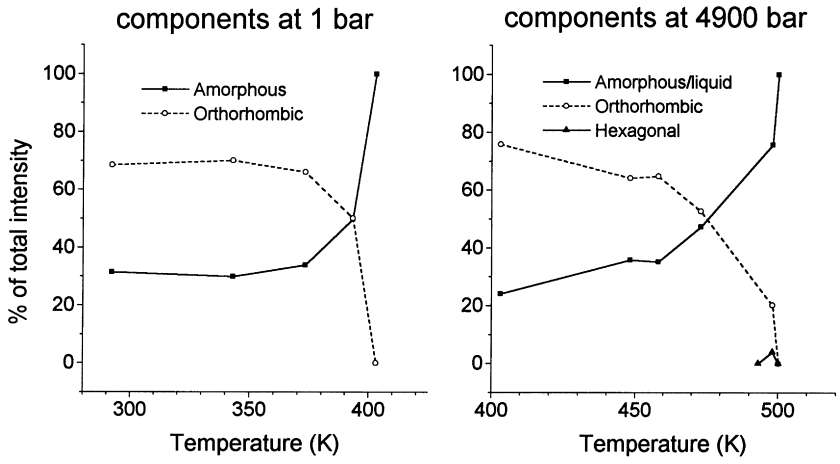

Fig. 8. Temperature dependence of the relative intensities of the line shape components in the deuterated FCC PE sample at 1 bar (left) and at 4900 bar (right).

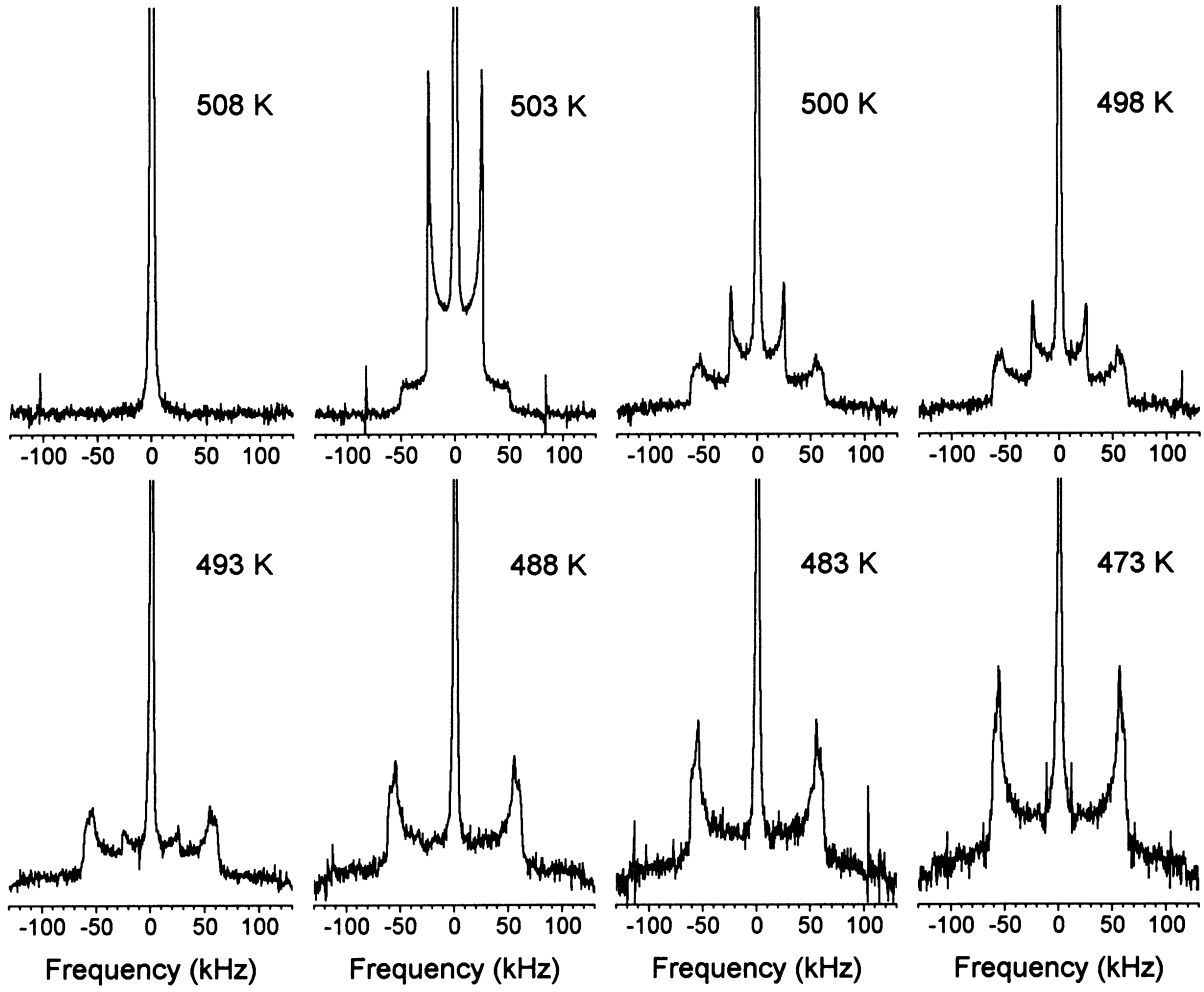

Fig. 9. Temperature dependence of deuteron NMR spectra at 4900 bar for ECC PE during the second run (at decreasing temperature).

agreement with similar phase diagrams derived from X-ray [3], DTA/DSC [1,2,35,36] and dilatometric [2] experiments.

3.2. Phase transitions studied using deuteron NMR spectra

The line shapes observed in deuteron NMR spectra allow us to distinguish between crystalline and amorphous parts and orthorhombic or hexagonal crystals. Therefore they may be used to perform a study on the changes in the fractions of the various components of the sample with temperature. Deuteron NMR line shapes obtained in the orthorhombic phase as a function of temperature at ambient pressure are shown in Fig. 7. A characteristic spectrum consists of a Pake doublet caused by the crystalline parts of the sample, combined with some additional intensity in the middle of the spectrum, which is due to the amorphous part of the sample. In this paper, we focus our attention to the changes in the various fractions with temperature and pressure. We will leave a more detailed discussion of these spectra to the next two papers [4,5].

In order to determine the fractions of crystalline and amorphous components, the contribution to the spectrum of the crystalline parts was fitted with calculated Pake line shapes. This contribution was then subtracted from the experimental spectrum to obtain a separate line originating from the amorphous parts of the sample. Subsequently both the crystalline and amorphous contributions to the line shape were integrated in order to obtain their relative contributions to the total spectrum. The results of this analysis at ambient pressure are shown on the left in Fig. 8. It appears that the crystallinity remains about constant at about 67% up to 373 K and then decreases until the melting transition is reached. This same result has also been obtained by Hentschel et al. [19], showing that our spectra and method of analysis can be compared very well with theirs.

The interesting part is of course to perform a similar analysis at high pressure and to investigate the behaviour in the vicinity of the hexagonal phase. As will be shown in our paper on the hexagonal phase [5], the deuteron NMR spectrum obtained in the hexagonal phase is similar to that in the orthorhombic phase, showing clearly, the amorphous and crystalline components. However, as the width of the hexagonal crystalline Pake doublet is less than half of that caused by the orthorhombic crystalline component it is also

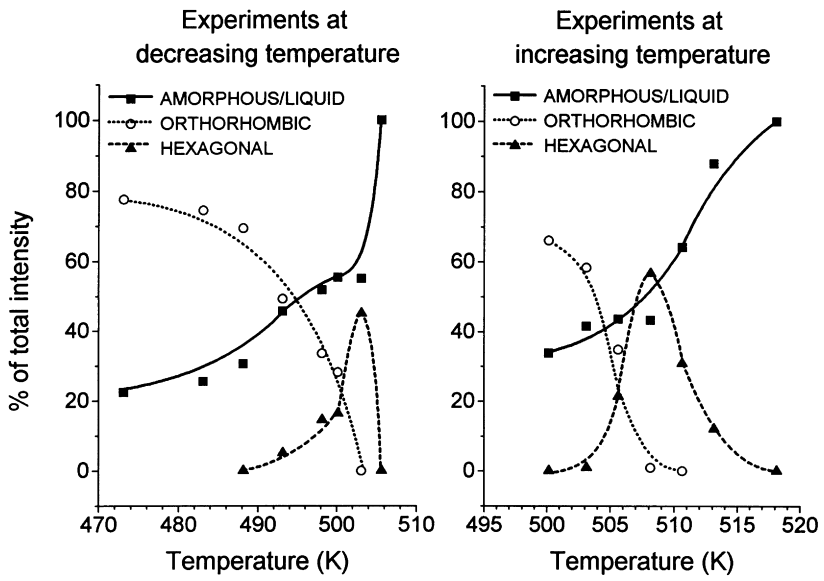

Fig. 10. Temperature dependence of the line shape component intensities at 4900 bar for deuterated ECC PE.

possible to clearly distinguish these two crystal structures. One can see that very well in Fig. 9, showing deuteron NMR spectra at 4900 bar. At some temperature values, all components coexist and show up as characteristic features in the recorded spectra.

The changes in the various fractions of the sample as a function of temperature were measured in three consecutive runs, showing the behaviour under distinctly different circumstances. In the first run at 4900 bar, a sample of deuterated PE crystallized at ambient pressure was used. In such a sample, the PE has a folded chain crystal (FCC) structure. During this run, temperature was increased step-by-step while monitoring the sample properties using various deuteron NMR experiments. In this way the transition from the orthorhombic phase to the hexagonal phase and the melting transition was observed.

The second run followed right after the first one, using the same sample, but this time the temperature was decreased from 523 K (in the liquid phase) to 473 K (in the orthorhombic phase). The temperature was lowered in small steps, making sure that the system could stabilize before each NMR experiment in order to obtain equilibrium state data. Of course, complete equilibrium cannot be achieved in practice due to the very long crystallization times. Our requirement here is that at each temperature value the NMR signals obtained do not change during the experiments. An indication that real equilibrium is not achieved is reflected in the observation that the phase transitions occur at different values of the temperature depending on whether the temperature is increased or decreased. The PE that is crystallized at high pressure through the hexagonal phase acquires the extended chain (ECC) structure. Therefore, the results obtained from the second run reflect the properties of ECC PE during crystallization. The third run, which involved increasing the temperature again, still using the same sample, was found to show clearly the temperature dependence of the different fractions in the sample for ECC PE, so comparisons to the FCC material can be made.

The analysis of the contributions of the crystalline and amorphous components of the sample was made in a similar way as above. One should note here that since it is not possible to distinguish between contributions from amorphous parts of the sample and signal originating from liquid material—in both of these phases C–D bonds perform fast isotropic motion—statements about either of these fractions always refer to the same features of the deuteron NMR spectrum.

Results of the analysis for FCC PE at 4900 bar are shown on the right hand side in Fig. 8. It appears that just like in the FCC material that was analysed at ambient pressure, here the crystallinity remains about 65% up to about 30 K below the phase transition. The apparent higher intensity of the rigid part (75%) measured at 400 K reflects the fact that high pressure reduces the mobility in the amorphous fraction to such an extent that frequencies in the slow tail of the distribution of motional frequencies in that fraction are no longer fast compared to the width of the spectrum. Therefore, part of the amorphous fraction contributes to the intensity of the rigid Pake line shape at this temperature. What may be a surprising result is that apparently, for FCC PE, the hexagonal phase coexists with the orthorhombic phase almost up to the melting point, and that the amount of hexagonal material is not very large (about 4% of the total signal).

Fig. 9 shows the temperature dependence of the deuteron NMR spectra at 4900 bar at decreasing temperature during the second run. At 508 K the spectrum consists of the narrow line obtained in the liquid phase. After passing the phase transition, the narrow Pake doublet, which is the

characteristic for the hexagonal phase, shows up very clearly in the spectrum at 503 K. An interesting effect is that on further decreasing the temperature to 500 K the wide Pake doublet due to the orthorhombic phase is observed at the same time. The orthorhombic component grows at the expense of the hexagonal component until, at 488 K, all hexagonal material has disappeared.

When we record the line shapes at increasing temperature starting in the orthorhombic phase, there is only one point, exactly on the phase transition temperature (505 K), where coexistence is observed. In the temperature range of the hexagonal phase (up to 513 K) all the observed crystalline material is exclusively hexagonal. The rest is due to the mobile amorphous or liquid fractions.

For ECC PE, the temperature dependence of the various fractions at 4900 bar is shown in Fig. 10. A difference between the ECC PE and the FCC material is that the phase transitions of ECC PE occur about 8 K higher than those for the FCC at 4900 bar. This reflects the increased thickness of the crystalline lamellae of PE when crystallized in the hexagonal phase. This increased crystallinity is also observed directly. At 473 K, FCC PE is only 50% crystalline, while the ECC material already shows a crystallinity of about 77%.

4. Conclusions

We have demonstrated that the NMR is a useful tool for studying phase transitions in PE also at high pressure. For the first time NMR techniques were used to determine the full phase diagram. In addition we have followed the changes of the orthorhombic crystalline, the hexagonal crystalline and the amorphous/liquid fractions of the material as a function of temperature and pressure. The temperature dependence of these fractions at ambient pressure is in good agreement with the behaviour found in the literature. At high pressure the behaviour is found to be similar, but shows differences between FCC and ECC material. The observed difference in melting temperature at 4900 bar between ECC PE and FCC PE is found to be about 8 K.

References

[1] Bassett DC, Turner B. Phil Mag 1974;29:285.
[2] Bassett DC, Turner B. Phil Mag 1974;29:925.
[3] Bassett DC, Block S, Piermarini GJ. J Appl Phys 1974;45:4146.
[4] de Langen M, Luigjes H, Prins KO. Polymer 2000;41:1183.
[5] de Langen M, Luigjes H, Prins KO. Polymer 2000;41:1193.
[6] Rempel RC, Weaver HE, Miller RL. J Appl Phys 1957;28(10):1082.
[7] Kitamaru R, Horii F. Adv Polym Sci 1978;26:139.
[8] Edzes HT, Bernards JPC. J Am Chem Soc 1984;106:1515.
[9] VanderHart DL, Khoury F. Polymer 1984;25:1589.
[10] Schmidt-Rohr K, Spiess HW. Macromolecules 1991;24:5288.
[11] Robertson MB, Ward IM, Klein PG, Packer KJ. Macromolecules 1997;30:6893.
[12] Punkkinen M, Ingman LP. Phys Stat Sol 1978;46:213.
[13] Rosenke K, Sillescu H, Spiess HW. Polymer 1980;21:757.
[14] Opella SJ, Waugh JS. J Chem Phys 1977;66(11):4919.
[15] Hentschel D, Sillescu H, Spiess HW. Macromolecules 1981;14:1605.
[16] Bridges BJ, Charlesby A, Folland R. Proc Roy Soc Lond 1979;A367:343.
[17] Alamo RG, Viers BD, Mandelkern L. Macromolecules 1995;28:3205.
[18] Hentschel D, Sillescu H, Spiess HW. Makromol Chem 1979;180:241.
[19] Hentschel D, Sillescu H, Spiess HW. Polymer 1984;25:1078.
[20] Kulik AS, Prins KO. Polymer 1994;35(11):2307.
[21] Odajima A, Sauer JA, Woodward AE. J Phys Chem 1962;66:718.
[22] Kitamaru R, Horii F, Zhu Q, Bassett DC, Olley RH. Polymer 1994;35(6):1171.
[23] Havens JR, VanderHart DL. J Magn Res 1985;61:389.
[24] Tzou DL, Schmidt-Rohr K, Spiess HW. Polymer 1994;35(22):4728.
[25] McBrierty VJ, McDonald IR. Polymer 1975;16:125.
[26] de Langen M, Prins KO. Rev Sci Instrum 1995;66:5218.
[27] Bunn CW. Trans Farad Soc 1939;35:482.
[28] Bunn CW. In: Renfrew P, Morgan P, editors. Polythene, ch. 5. London: Iliffe, 1960.
[29] McCrum NG, Read BE, Williams G. Anelastic and dielectric effects in polymeric solids. New York: Dover, 1991.
[30] Wunderlich B. Macromolecular physics. Crystal structure, morphology, defects, 1. New York: Academic Press, 1973.
[31] Edzes HT, Bernards JPC. J Am Chem Soc 1984;106:1515.
[32] Schmidt-Rohr K. Multidimensional solid-state NMR and polymers. New York: Academic Press, 1994.
[33] Klein PG, Robertson MB, Driver MAN, Ward IM, Packer KJ. Polym Int 1988;47:76.
[34] Yasuniwa M, Enoshita R, Takemura T. Jap J Appl Phys 1976;15:1421.
[35] Hikosaka M, Minomura S, Seto T. Jap J Appl Phys 1980;19(6):1763.
[36] Hikosaka M, Tsukijima K, Rastogi S, Keller A. Polymer 1992;33(12):2502.